16th World Conference on Earthquake Engineering, 16WCEE 2017
Santiago Chile, January 9th to 13th 2017
Paper N° 2613
Registration Code: S-B1463198334

Potential for Damage to Brittle Structures in Induced Earthquakes

R.E. Chase[(1)], A.B. Liel[(2)]

[(1)] Graduate Student Researcher, Department of Civil, Environmental and Architectural Engineering, University of Colorado Boulder, robert.chase@colorado.edu
[(2)] Associate Professor, Department of Civil, Environmental and Architectural Engineering, University of Colorado Boulder, abbie.liel@colorado.edu

Abstract

In this study, damage to built infrastructure from induced earthquakes is investigated through nonlinear dynamic structural response simulations. These simulations are based on a typical brick residential chimney. We focus on brick chimneys because they are ubiquitous and representative of brittle construction more generally. This study uses a finite element model of the chimney to develop a simpler macro model, which is subjected to ground motion recordings from induced events, including those in Arkansas, Kansas and Texas, as well as the Geysers geothermal field in California. The dynamic response of the models under induced motions is compared to the dynamic response from recordings of tectonic earthquakes with similar magnitudes and depths. Results are used to quantify differences in structural response through collapse and damage fragility curves, when the chimney is subjected to ground motions from tectonic versus induced events. The findings indicate the induced ground motions are less damaging than natural motions for a given intensity of shaking. This difference in response has been modestly correlated with the difference of significant durations in the ground motions and depth of rupture, and reflects differences in frequency content between induced and tectonic motions.

Keywords: induced seismicity; chimneys; damage; collapse; central and eastern U.S.

1. Introduction

Earthquakes have generally been thought of as a natural occurrence, caused by underlying tectonic movement, a gradual build up stresses over time and eventual slip, releasing the stored strain energy and causing an earthquake [1]. However, earthquakes at the Rocky Mountain Arsenal near Denver, Colorado in the 1960s raised awareness that human-caused earthquakes could occur, and damage built infrastructure [2, 3]. Denver had no history of significant earthquakes until 1967, when seismic swarms began, eventually culminating with three events with magnitude greater than 5.0. These events were linked to underground disposal of chemical-waste by the U.S. Army, by observing correlations between injection rate and earthquake occurrence [2]. Since the Rocky Mountain Arsenal earthquakes, hundreds of human-caused earthquakes have been observed. Much of this induced seismicity has been linked to various forms of energy development, including deep wastewater injection/disposal, enhanced geothermal systems, hydraulic fracturing, hydrocarbon withdrawal, reservoir impoundment, and carbon capture and storage [2].

Deep wastewater disposal is thought to be primarily responsible for the uptick in induced seismicity currently occurring in the central and eastern United States (CEUS) [4, 5], which affects Oklahoma, Colorado, Arkansas, Kansas, Texas, and Ohio, among other states. This wastewater is a byproduct of oil and natural gas extraction processes, including fracking, and is disposed of by Class II injection wells, which dispose of the water underground [6]. This reinjection can cause earthquakes by increasing pore pressures and decreasing frictional resistance, thereby increasing the potential for seismic slippage [7]. Recent studies have shown that wastewater-related seismicity correlates with the volume and pressure of fluids injected [2]. However, among thousands of deep wastewater injection wells across the U.S. [2], only about 10% of all Class II injection wells have found to be associated with earthquakes [5]. To complicate matters further, injection rates can change dramatically as a function of fossil fuel demand and other economic and regulatory factors.

Damage experienced in the U.S. recent earthquakes suggests the need to re-evaluate the conventional wisdom, which holds that injection-induced earthquakes are not large enough to cause significant damage to

buildings and infrastructure. There have now been dozens of earthquakes in Oklahoma alone that have been associated with damage to structural or nonstructural components of buildings. This damage has been associated with millions of dollars of insurance claims and is the subject of a major class action lawsuit. In addition, as a result of the damage and fears of induced seismicity, preliminary mitigation measures have been taken in some places. For example, following a significant increase in seismicity in 2014 and the beginning of 2015, the Kansas Corporation Commission (responsible for regulation of oil and gas development in that state) ordered reductions in volume and pressure of injected wastewater at multiple injection wells in the southern part of the state "to protect the public from immediate danger to health, safety, and welfare" [8]. Likewise, earthquake swarms occurring on the Guy-Greenbrier Fault in central Arkansas led to the eventual shut down and plugging of four Class II injection wells that were suspected of causing the major earthquakes [6]. Oklahoma has also changed regulations to attempt to reduce shaking.

This study examines induced ground motions and the potential damaging effects they can have on the existing built environment. Little is known about the impacts of ground motions from induced earthquakes on structures and how induced earthquakes may affect structures similarly or different from tectonic events. This study focuses on residential building chimneys because of the significant damage these structures, like that shown in Fig. 1, have experienced in induced events in recent years (including, but not limited to, those in Love County, Edmonds, Prague and Crescent, Oklahoma). To explore the relationship between ground shaking from induced earthquakes and damage, we first collect a suite of ground motion recordings from induced earthquakes, as well as similar tectonic (not induced) ground motions that are suitable for engineering analysis. We then build a nonlinear simulation model of the chimney's structural response. Both the induced and tectonic ground motions are applied to the chimney model, quantifying chimney collapse and damage probabilistically and comparing these responses under the induced and tectonic ground motion sets. The results are analyzed to determine trends relating damage to ground motion characteristics. The ultimate goal is to assess if induced ground motions present different risks to consider from natural, tectonic earthquakes, and to quantify the fragility of typical residential chimneys in both cases.

2. Ground Motion Selection

First, acceleration recordings from induced and tectonic earthquakes were obtained for use in subsequent structural analysis. The motions were gathered from online databases of ground motion recordings, such as IRIS, the Center for Engineering Strong Motion Data, the Northern California Earthquake Data Center, and the PEER NGA-East Ground Motion Database [9, 10, 11, 12].

2.1 Induced ground motion set

Induced ground motions were selected from different confirmed induced events across the United States. These "confirmed" events are generally accepted as induced, *i.e.* originating from human activities, by the scientific community. To select ground motions, candidate confirmed events were gathered from published studies by academics, government agencies, and others. We considered events occurring in the 14 designated areas of non-tectonic seismicity by the USGS [13], as well seismic activity in the Geysers and Coso geothermal fields in California. In this analysis, induced motions are not distinguished between those from geothermal fields and those from wastewater disposal, due to limitations in available data in the CEUS region, which has historically had sparse seismic instrumentation. Priority was given to the selection of motions from larger magnitude events, because they were more widely felt [14], and more likely to cause damage to structures. In addition, we focused on gathering ground motions with larger peak ground accelerations (PGA) and peak ground velocities (PGV).

Fig. 1 – Collapsed chimney caused by the M_W 5.7 2011 Prague, Oklahoma Earthquake [15].

Table 1 provides a complete list and description of the 30 induced motions, which includes events from the Geysers and Coso Geothermal Fields in California, the Guy-Greenbrier Fault in Arkansas, Oklahoma, Timpson, TX, and in southern Kansas. The ground motions are from earthquakes ranging in (moment) magnitude from 3.6 to 5.7, and occurred at an average rupture depth of 4.15 km. All records were filtered using a Butterworth filter and baseline corrected.

Table 1 – Ground motions from induced earthquakes, with summary characteristics.

#	Location	Date	Mag. (M_W)	Depth (km)	PGA (g)	PGV (cm/s)	Sa(0.3s) (g)
1	The Geysers, CA	1/12/2014	4.5	2.6	0.20	6.14	0.22
2	The Geysers, CA	4/24/2007	4.4	2.5	0.30	7.08	0.40
3	The Geysers, CA	8/3/2003	4.2	0.9	0.07	1.20	0.05
4	The Geysers, CA	1/4/2009	4.2	4.7	0.17	4.11	0.31
5	The Geysers, CA	7/15/2010	4.0	2.9	0.16	4.24	0.16
6	The Geysers, CA	2/28/2011	4.5	3.0	0.20	5.43	0.22
7	The Geysers, CA	3/31/2012	3.5	1.4	0.17	3.55	0.10
8	The Geysers, CA	5/5/2012	4.5	2.8	0.11	3.00	0.20
9	The Geysers, CA	5/13/2012	3.9	3.5	0.01	0.25	0.02
10	The Geysers, CA	7/8/2012	3.8	3.9	0.13	2.87	0.12
11	The Geysers, CA	3/14/2013	4.5	2.2	0.22	5.35	0.20
12	The Geysers, CA	1/21/2014	3.6	2.5	0.03	0.84	0.03
13	Coso, CA	1/15/2010	4.4	7.0	0.05	2.89	0.10
14	Coso, CA	12/23/2013	4.3	2.1	0.06	1.93	0.13
15	Timpson, TX	1/25/2013	4.1	5.0	0.57	20.3	0.92
16	Timpson, TX	9/2/2013	4.2	4.8	0.17	5.95	0.19
17	Timpson, TX	9/2/2013	4.3	4.7	0.11	3.83	0.16
18	The Geysers, CA	7/9/2015	3.8	3.9	0.14	3.02	0.41
19	Southern Kansas	10/2/2014	4.4	5.0	0.19	2.59	0.12
20	Greenbrier, AR	2/28/2011	4.7	10.0	0.05	1.59	0.04
21	Guy, AR	10/15/2010	3.9	7.5	0.03	0.39	0.01
22	Guy, AR	11/20/2010	3.9	2.8	0.02	0.57	0.02
23	Prague, OK	11/6/2011	5.7	3.1	0.03	1.26	0.04
24	Crescent, OK	7/27/2015	4.5	5.0	0.01	0.22	0.01
25	Norman, OK	10/13/2010	4.3	4.8	0.01	0.25	0.01
26	Edmond, OK	12/29/2015	4.3	6.1	0.32	5.87	0.18
27	Timpson, TX	1/25/2013	4.1	5.0	0.37	20.1	0.72
28	Timpson, TX	9/2/2013	4.2	4.8	0.10	4.00	0.18
29	Timpson, TX	9/2/2013	4.3	4.7	0.11	2.97	0.14
30	Conway Springs, KS	11/12/2014	4.8	5.4	0.08	2.26	0.06
		Median	**4.3**	**4.3**	**0.11**	**2.98**	**0.13**

2.2 Tectonic ground motion set

Tectonic ground motions were chosen to have similar characteristics to the selected induced motions. Major parameters that factored into their selection include earthquake magnitude and rupture depth, and ground motion PGA and PGV. The tectonic ground motions are from earthquakes ranging in (moment) magnitude from 2.8 to 6.0, similar to the induced events, and at an average rupture depth of 12.7 km, deeper than those in the induced ground motion set. The tectonic motions have somewhat lower PGAs than their induced counterparts; work is ongoing to expand this record set.

Table 2 – Ground motions from tectonic earthquakes, with summary characteristics.

#	Location	Date	Mag. (M_W)	Depth (km)	PGA (g)	PGV (cm/s)	Sa(0.3s) (g)
1	Napa, CA	8/24/2014	6.0	11.3	0.98	22.1	1.39
2	Westmorland, CA	4/26/1981	5.9	2.3	0.38	44.1	0.77
3	Mammoth Lakes, CA	1/7/1983	5.3	3.0	0.16	17.3	0.38
4	Imperial Valley, CA	10/16/1979	5.6	3.3	0.11	12.0	0.18
5	Mt. Carmel, IL	4/18/2008	4.6	14.0	0.034	0.88	0.063
6	Mineral, VA	8/23/2011	5.7	7.5	0.062	0.24	0.007
7	Miramichi, NB	3/31/1982	4.5	5.0	0.41	3.18	0.069
8	Riviere Du Loup, QC	3/6/2006	4.7	13.0	0.040	0.67	0.012
9	Saguenay, QC	11/25/1988	5.9	26.0	0.092	2.99	0.20
10	Mt. Carmel, IL	4/18/2008	5.3	15.7	0.002	0.05	0.0034
11	Val Des Bois, QC	6/23/2010	5.1	18.7	0.018	0.20	0.0099
12	Sullivan, MO	6/7/2011	3.9	27.0	0.002	0.03	0.0009
13	La Malbaie, QC	6/13/2003	3.5	10.3	0.029	0.44	0.010
14	Slaughterville, OK	10/13/2010	4.4	14.0	0.012	0.31	0.024
15	Baie St. Paul, QC	4/7/2006	3.7	25.0	0.012	0.12	0.002
16	Cap Rouge, QC	11/6/1997	4.5	21.7	0.0003	0.02	0.0006
17	Miston, TN	6/2/2005	4.0	15.0	0.0022	0.08	0.0056
18	Thurso, QC	2/25/2006	3.7	17.5	0.0018	0.04	0.0025
19	Shady Grove, AR	5/1/2005	4.3	8.0	0.0111	0.55	0.0198
20	Au Sable Forks, NY	4/20/2002	5.0	10.0	0.0115	0.52	0.0257
21	Hawkesbury, ON	3/16/2011	3.6	7.5	0.0067	0.05	0.0013
22	Buckingham, VA	6/11/2008	3.0	18.0	0.0003	0.00	0.0001
23	Marston, MO	10/18/2006	3.4	8.2	0.0036	0.10	0.0037
24	Charlevoix, QC	5/22/2001	3.6	11.4	0.0039	0.05	0.0010
25	Whiting, VT	3/2/2010	3.4	5.0	0.0043	0.08	0.0059
26	Ft Payne, AL	4/29/2003	4.6	12.0	0.0032	0.08	0.0062
27	Bark Lake, ON	10/12/2003	3.8	18.0	0.0036	0.02	0.0013
28	Charleston, SC	11/11/2002	4.0	9.0	0.0031	0.05	0.0063
29	Cobourg, ON	7/19/2007	2.8	5.0	0.0021	0.01	0.0002
30	Caborn, IN	6/18/2002	4.6	17.5	0.0021	0.15	0.0053
		Median	**4.4**	**11.7**	**0.01**	**0.14**	**0.01**

3. Chimney Modeling

3.1 Chimney characteristics

This study examines the performance of a residential masonry chimney that is representative of those that have been damaged in induced events (e.g. Fig. **1**). These unreinforced brick chimneys are commonplace in regions that do not see frequent seismic activity. For the purpose of this investigation, the chimney is based on typical chimney dimensions as defined by [16], and shown in Fig. 2 (a). The chimney is assumed to be constructed of red clay brick with typical mortar. This masonry construction was also assumed to be unreinforced and unconfined. The anchorage between the house and the chimney in these regions is not substantial and is assumed not to significantly impact structural response. The total mass of the chimney is approximately 4900 kg.

3.2 Finite element model and calibration

The chimney was first modeled in two-dimensions in the finite element software ABAQUS [17]. The material properties of the chimney are represented by a homogenous isotropic material that represents the aggregate response of clay bricks, mortar between the bricks, and interface between the materials. A model that separately characterizes the brick, mortar, and interface between the materials may more accurately capture the response of the chimney in a seismic event, by capturing failure mechanisms associated with shear sliding along the mortar joints and tensile cracking and compressive crushing of the brick and mortar. However, these models are too computationally intensive for this study. Thus, the more basic isotropic material model was chosen for the chimney, and calibrated to match the response of masonry construction. This modeling approach has been used in a number of studies, and Lourenco [18] and others have shown that reasonable results can be obtained.

(a) ABAQUS (b) OpenSees

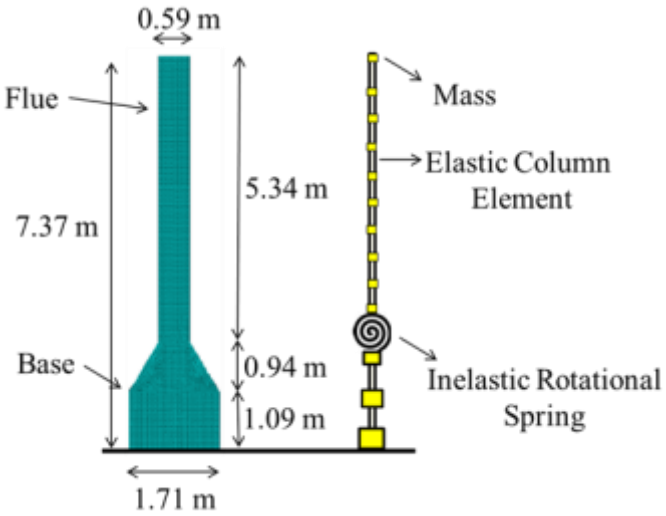

Fig. 2 - Chimney dimensions, as represented in (a) finite element (ABAQUS). The macro (OpenSees) model is shown in (b) for comparison.

The ABAQUS Concrete Damaged Plasticity (Fenves-Lee) model is adopted as the material model for the homogenous isotropic material in the chimney. The Concrete Damaged Plasticity Model is intended for brittle materials such as concrete, masonry, and brick. Fig. 3 shows the monotonic backbone of the tensile and compressive responses for this model. Compressive plasticity is modeled in accordance with Lourenco [18]. The model exhibits nonlinear compressive softening curve to represent the softening behavior of a brittle material such as masonry in compression. In compression, the model is defined by an initial nonlinear region before the ultimate stress is reached, and a second softening region described by the compressive fracture energy. The tensile plasticity model was also taken from Lourenco [18]. This model describes the loss of strength as the material fails in tension based on the tensile fracture energy, which is the area under the nonlinear, post elastic curve. Lourenco [18] has shown that this model can describes the tensile softening behavior of a brittle material such as masonry.

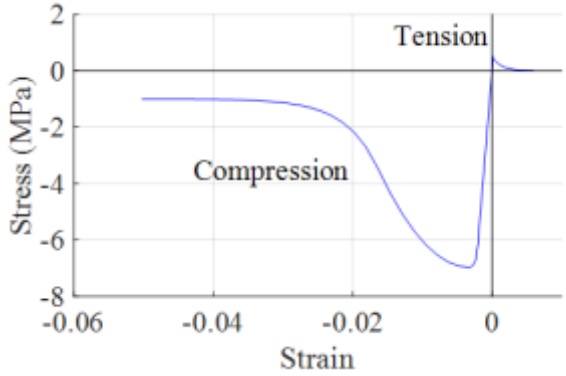

Fig. 3 – Stress-strain relationship used to model homogenous chimney material in ABAQUS, demonstrating response in for tension and compression.

To determine the material parameters, a brick masonry wallette specimen tested and simulated by Lourenco [18] was modeled in ABAQUS by the authors. The brick and mortar of the chimney is assumed to be similar to the material of the wallette specimen. The material properties of the masonry material described above were adjusted to most closely match the numerical results reported by Lourenco [18], focusing on capturing the base shear versus top displacement curve reported, as well as to attain the diagonal propagating crack as the failure mechanism. The force-displacement curves from the two studies are provided in Fig. 4 (a), showing that the ABAQUS model reasonably reproduces the response of the masonry unit. The failure mechanisms also show good agreement, as shown in Fig. 4 (b).

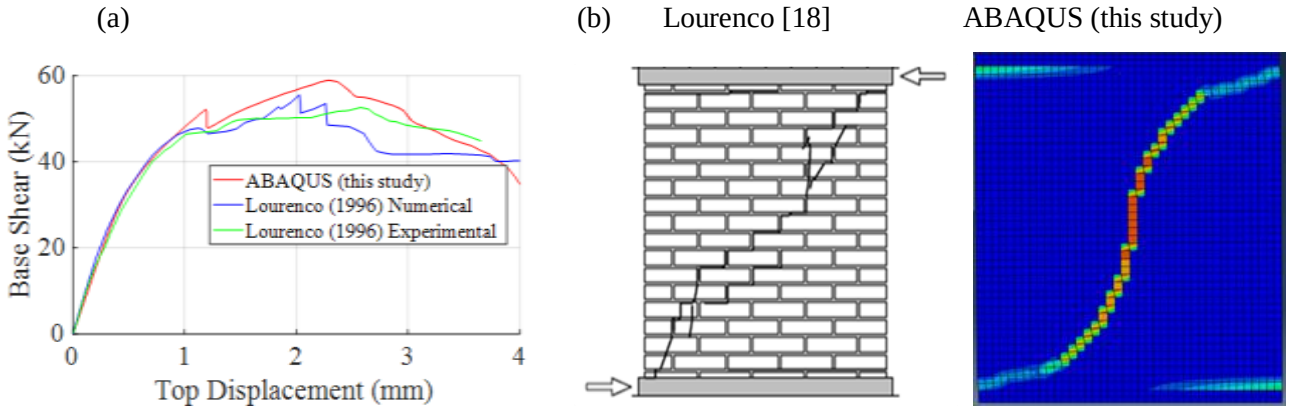

Fig. 4 – Comparison of our ABAQUS model of a wallette specimen with previous work Lourenco [18], showing (a) force-displacement response and (b) diagonal crack propagation for an experimental specimen from [18] and this study. In (b) the colors represent the plastic tensile strain with red and orange being the largest values. The figure from [18] in (b) is taken directly from that publication.

This material model was applied to the chimney configuration shown in Fig. 2 (a). The ABAQUS model was then subjected to a pushover analysis under a distributed displacement along the length of chimney, illustrated in Fig. 5. The failure mode was characterized by a tensile crack that opened at the joint between the flue and base of the chimney, and subsequent crushing the masonry.

3.3 OpenSees macro model

The ABAQUS model was used as the basis for a more computationally-efficient model developed in the opensource OpenSees platform [19]. As shown in Fig. 2 (b)**Error! Reference source not found.**, the OpenSees model consists of elastic elements with mass concentrated at 16 nodes throughout its length. The model has a single spring located at the base of the flue concentrating the nonlinear response. The spring is assigned the "hysteretic" material model in OpenSees, which has trilinear monotonic backbone. This spring placement mimics

the predominant failure mechanism of the ABAQUS chimney, in which a cracked formed at the joint of the upper shaft (flue) and lower base of the chimney. This macro modeling approach allows for more extensive analysis techniques such as incremental dynamic analysis (IDA) which was utilized in this study.

The OpenSees model was designed to be a reasonable representation of the more detailed ABAQUS model. The model was calibrated to exhibit similar responses in terms of natural frequency, and static pushover response (displacements, base shear, and failure mechanisms). Initially, the model was calibrated to the elastic response of the finite element model using the Youngs modulus of the homogenous material and the moment of inertia of the chimney cross section. Once the elastic parameters were determined, the nonlinear spring was calibrated to govern the rest of the nonlinear response. Both models were subjected to a static pushover analysis which consisted of triangular distributed load along the chimney height. The force-displacement curve for both analyses is illustrated in Fig. 5, showing good agreement between the two modeling approaches. In addition, the natural period of the OpenSees chimney model was calibrated to be a close as possible to the ABAQUS model. The ABAQUS natural period was determined to be 0.34 seconds, while the OpenSees model had a natural period of 0.26 seconds. Differences can be attributed to the lumped mass and stiffnesses in the OpenSees model. Damping in the Opensees model was applied with 5% Rayleigh damping at the first and third mode considering tangent (updated) stiffness.

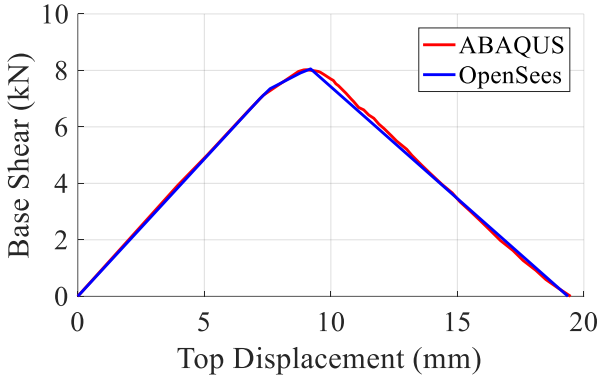

Fig. 5 – Pushover results from finite element (ABAQUS) and macro (OpenSees) models.

4. Chimney Seismic Response

4.1 Incremental dynamic analysis results

Incremental dynamic analysis was applied to the OpenSees chimney model to quantify its seismic response. Incremental dynamic analysis is implemented by scaling up a ground motion while recording the structure's response (such as drift or displacement) against intensity parameters (such as spectral acceleration or PGA). The intensity parameters are increased, ground motion scaled, and structural response repeated until the structure fails or collapses as defined by the user. The process is repeated for multiple ground motions to quantify the record-to-record variability in the response [20]. Here, the IDA was run for the 30 induced motions and then, separately, for the 30 tectonic motions to permit comparison between the responses.

In this study, chimney collapse was defined as occurring when the top displacement of the chimney reached 19.5 mm. This point corresponds to the top displacement at which the base shear of the structure is zero in the pushover analysis (Fig. 5), signaling that the chimney has lost all of its lateral capacity. Significant damage was assumed to occur if the top displacement reached 11.3 mm, corresponding to the post-peak point in the pushover at which the structure has lost 20% of its strength. The ground motion intensity used in IDA is defined as the spectral acceleration of the record at the first mode period of the chimney, SA(T= 0.3s), considering 5% damping.

The resulting IDA curves are shown in Fig. 6, with different colored lines for each of the distinct ground motion records. The black line is the median IDA of the 30 motions in each set. Comparing the IDA results for the tectonic and induced ground motions, there is (unsurprisingly) very good agreement when the chimney response is in the elastic range (approximately below 8 mm of top displacement, which is consistent with the

pushover results in Fig. 5). Once the top displacement exceeds 8 mm, the response becomes more nonlinear. In both cases when the top displacement exceeds about 10 mm, the response becomes highly nonlinear.

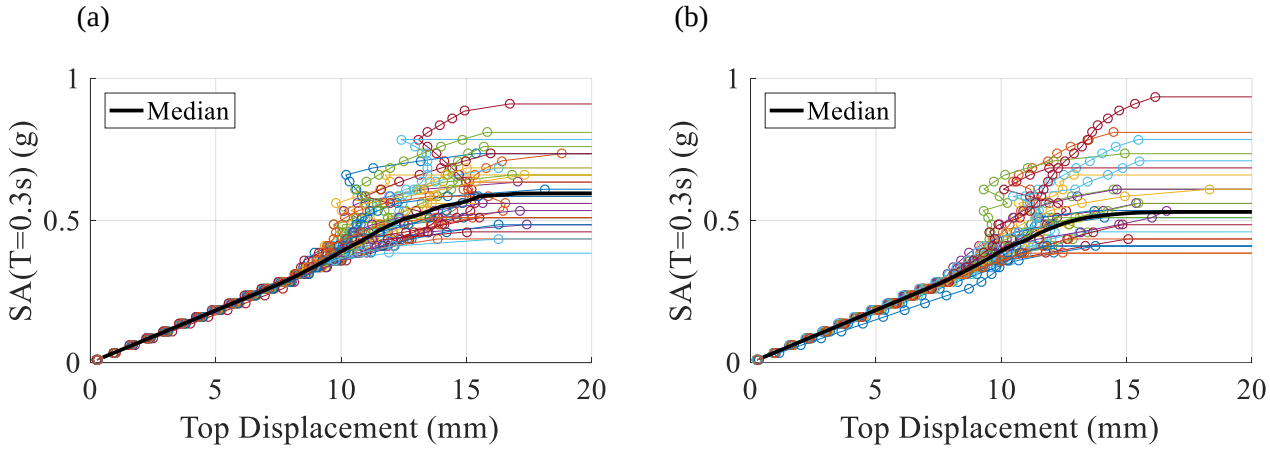

Fig. 6 – IDA results when chimney is subjected to (a) induced and (b) tectonic ground motion sets. The black line represents the median response of the set.

4.2 Fragility curves

To summarize the IDA results statistically, fragility curves were constructed. A fragility curve takes the ground motion intensity associated with chimney collapse (or damage) for all of the motions and constructs a cumulative density function of those values, representing probability of collapse (or damage) as a function of ground motion intensity. Following typical practice, a lognormal probability model was fit to the data. In this study, we constructed fragility curves separately for the results from induced and tectonic motions and considering two different measures of ground motion intensity at collapse: spectral acceleration and PGV. The collapse fragilities are provided in Fig. 7. The statistics of the collapse fragility curves are provided in Table 3. Damage fragilities are also shown in Fig. 7 (a).

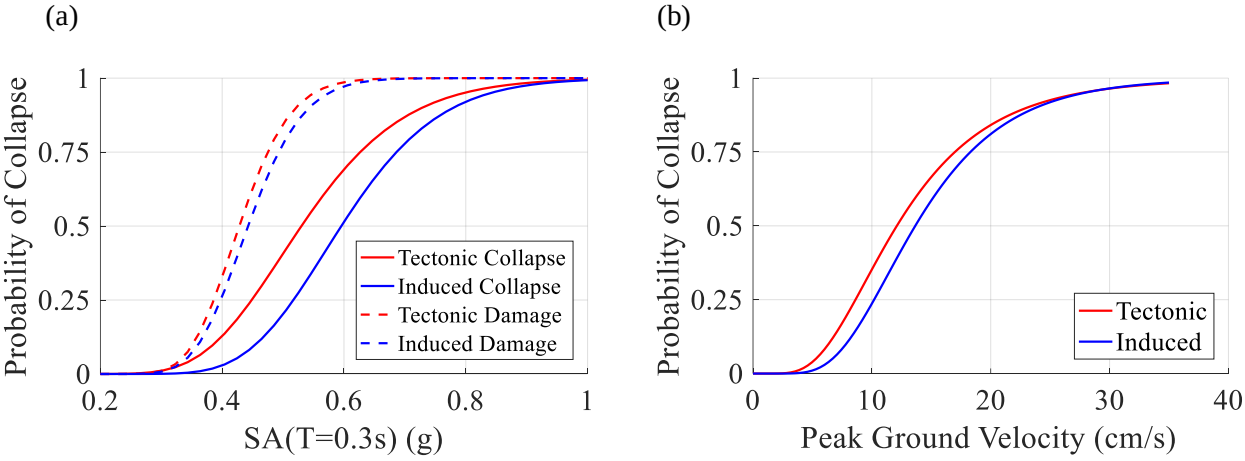

Fig. 7 – Collapse fragility curves for chimney, where ground motion intensity is quantified by (a) spectral acceleration and (b) peak ground velocity.

Fig. 7 shows that, regardless of intensity measure considered, the tectonic ground motion set has a higher probability of collapse for a given intensity of shaking. For example, the median collapse capacity, i.e. ground motion intensity corresponding to 0.5 probably of collapse, corresponds to a spectral acceleration of 0.52g at 0.3s given a tectonic event, and 0.6g for an induced event, about 13% different. Similarly, given a PGV of 15 cm/s

occurs, the probability of collapse for an induced event is 0.6, while the probability of collapse for a tectonic event for the same PGV is 0.67. The median chimney "damage" fragility is 3% less for the tectonic as compared to induced set. These trends suggest that induced events are less likely to incite the collapse of a chimney when compared to tectonic events, given the same intensity of shaking. Although previous researchers have suggested that PGV is a strong predictor of damage in induced events [21], the standard deviation of the collapse fragility curves is substantially less for the spectral acceleration based curve than the PGV curve, suggesting that spectral acceleration is a more efficient predictor of the structural response for the chimney model.

Fig. **8** also explores the induced earthquake collapse fragility further by separating the motions into two groups: ground motions from injection induced seismicity (15 of 30 motions), and ground motions triggered by enhanced geothermal systems (15 of 30 motions). For these motions, the geothermal motions are less damaging than then injection induced seismicity. The injection-triggered motions are less damaging at lower spectral values, but approach the tectonic events at larger levels of acceleration.

Table 3 – Statistics for collapse fragilities in terms of spectral acceleration at 0.3s and PGV.

Parameter	Collapse Sa Fragility (0.3s) (g)		Collapse PGV Fragility (cm/s)	
	Induced	Tectonic	Induced	Tectonic
Median	0.60	0.52	13.7	12.1
Ln Standard Deviation	0.21	0.25	0.43	0.50

4.3 Why do induced motions produce less damage?

These fragility results suggest that induced motions may produce less damage, as compared to a tectonic motion with comparable intensity. This finding is consistent with Hough [14], who used response to the USGS "Did you Feel it?" website to suggest that shaking intensity was less severe in induced events than expected based on the tectonic record for earthquakes of similar magnitude, at least for some cases. Here, we examine how characteristics of the ground motion or earthquake between the two motion sets may systematically explain these trends.

Examining first differences in ground motion characteristics between the two record sets, there is a notable difference in significant duration between the motions in the induced and tectonic sets. For our record sets, the mean significant duration, computed as the time during which 5 to 95% of the Arias Intensity is accumulated [22], for the induced records was 6.3 seconds, but 26.9 seconds for the tectonic motions. As has been demonstrated in other studies, e.g. [23], extended duration of shaking produces more cycles of vibration, and can cause failure at lower shaking intensities. Indeed, the chimney results here showed that there is some correlation between the spectral acceleration at collapse and the significant duration of the ground motion within a given ground motion set that may also explain differences between the sets. This correlation is strongest for enhanced geothermal ground motions ($R^2 = 0.18$), but can begin to describe why there is difference in structural response to induced as compared to tectonic earthquakes.

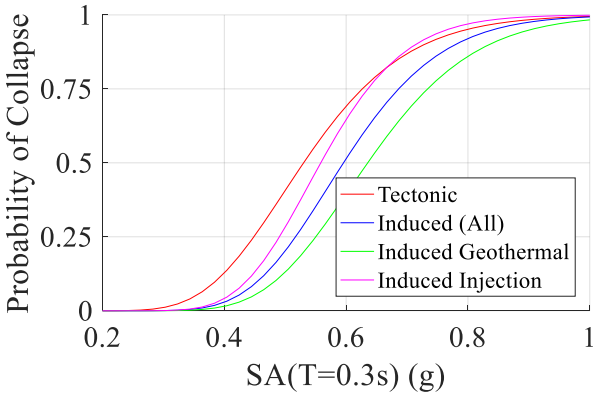

Fig. 8 – Collapse fragility curves comparing geothermal and injection-triggered motions.

In addition to differences in significant duration, the induced motions are also characterized by their high energy content at high frequencies (short periods). Fig. 9 shows the median response spectra for the induced and tectonic motion sets, where the response spectra of each of the records are scaled to the level causing collapse of the chimney. The induced spectra shows high energy (i.e. high spectral content) at short periods and then the energy dies out quickly for other, longer periods. The tectonic motion spectrum shows relatively lower energy for short periods. At the period of the chimney (0.26s) the collapse spectra for the induced motions are higher, signaling that induced motions require a higher spectral acceleration to cause collapse. If the tectonic spectra were to be scaled up to the same spectral acceleration as the induced at the period of the chimney, it would have stronger long period energy. This would have a greater influence on the chimney response as its period elongates due to cracking and damage.

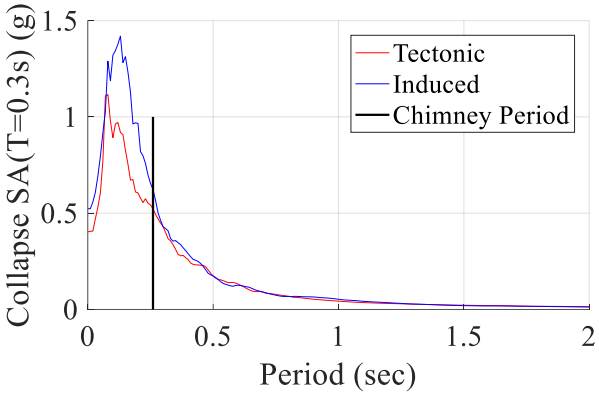

Fig. 9 – Median response spectra for tectonic and induced ground motion sets when motions are scaled to collapse.

Turning now to earthquake source characteristics, we investigate the sensitivity of the response to the depth of the earthquake. Depth is of interest because the tectonic set has generally deeper rupture depths than the induced set, and because Hough [14] previously identified the shallow depth and low stress drop of induced motions as potentially significant in terms of the damage observed. To explore the impacts of depth, we plotted the spectral acceleration at which collapse occurred against the depth of the record, as shown in Fig. **10**. These results show that among some of the subsets of records, depth is inversely related to collapse SA. The strongest trend is apparent for the enhanced geothermal motions. This dependence on depth seems to suggest that depth may explain some of the differences observed between induced and tectonic motions.

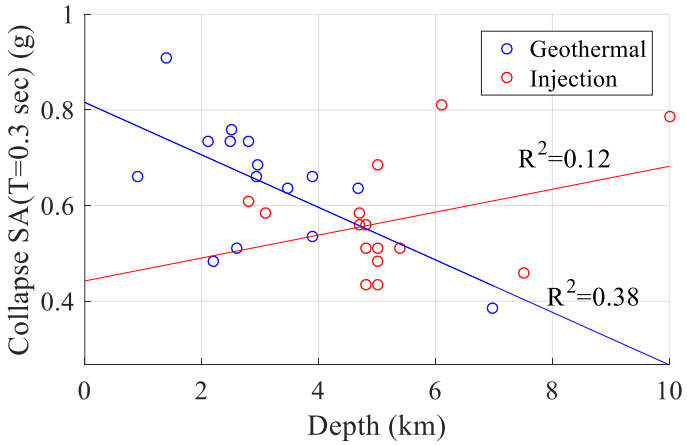

Fig. 10 – Scatterplot with trendlines of colllapse spectral acceleration vs depth for geothermal and injection induced earthquakes.

5. Conclusions

This study aims to quantify the differences in structural response under induced and tectonic ground motions to better evaluate the risk that these motions pose for built infrastructure. With the rapid increase in the number of induced earthquakes through the Central and Eastern United States, it is critical that the hazard presented by induced seismicity be investigated to further knowledge about the risk to existing infrastructure and what this means for future construction practices, insurance policies and other decisions.

To investigate the susceptibility of the built environment to induced earthquakes, this study quantifies the probability of collapse of a residential chimney subjected to both induced and tectonic earthquakes. The findings show that induced events produce a lower probability of collapse or damage than tectonic motions with the same intensity. In addition, preliminary results suggest that differences in the significant durations and the depths of rupture between the two likely contributed to the different responses observed. Differences in frequency content between the two suites of motions were also significant, with greater short period energy in the induced ground motion set.

The findings of this study are limited by the ground motions selected for the analysis which are affected by the limited number of ground motion recording available in the CEUS. Further work will be conducted to bolster these suites of motions to develop more representative and similar sets.

6. Acknowledgments

This material is based upon work supported by the National Science Foundation under Grant No. 1515438. Initial work was also funded by a University of Colorado Innovation seed grant. Any opinion, findings, and conclusions or recommendations expressed in this material are those of the authors(s) and do not necessarily reflect the views of the National Science Foundation. The authors would also to acknowledge the contributions of Jack Baker, Abhineet Gupta, Guido Camata, Taojun Liu, Nicolas Luco, Anne Sheehan, and Nicola Tarque.

7. References

[1] United States Geological Survey, "Reid's Elastic Rebound Theory," 18 July 2012. [Online]. Available: http://earthquake.usgs.gov/regional/nca/1906/18april/reid.php. [Accessed 5 February 2015].

[2] The National Research Council, "Induced Seismicity Potenial in Energy Technologies," National Academy of Sciences, Washington DC, 2012.

[3] J. Healy, W. Rubey, D. Griggs and C. Raleigh, "The Denver Earthquakes," *Science*, pp. 1301-1310, 1968.

[4] United States Geological Survey, "Induced Earthquakes," 1 January 2015. [Online]. Available: http://earthquake.usgs.gov/research/induced/. [Accessed 6 February 2015].

[5] M. Weingarten, S. Ge, W. Godt, B. Bekins and J. Rubinstein, "High-rate injection is associated with the increase in U.S. mid-continent seismicity," Science Magazine, Washington, DC, 2015.

[6] United States Environmental Protection Agency, "Minimizing and Managing Potential Impacts of Injection-Induced Seismicity From Class II Disposal Wells: Practical Approaches," United States Environmental Protection Agency, Washington, DC, 2014.

[7] C. Kisslinger, "A review of theories of mechanisms of induced seismicity," *Engineering Geology*, pp. 85-98, 1976.

[8] The State Corporation of the State of Kansas, "Order Reducing Saltwater Injection Rates," The State Corporation of the State of Kansas, 2015.

[9] Incorporated Research Institutions for Seismology, "IRIS," 2015. [Online]. Available: http://www.iris.edu/hq/. [Accessed 10 Feburary 2015].

[10] Center for Engineering Strong Motion Data, "CESMD," 2015. [Online]. Available: http://strongmotioncenter.org/. [Accessed 10 February 2015].

[11] Northern California Earthquake Data Center, "NCEDC," 13 January 2015. [Online]. Available: http://quake.geo.berkeley.edu/. [Accessed 10 February 2015].

[12] Pacific Engineering Earthquake Research Center, "PEER NGA-East Ground Motion Database," PEER, 2016. [Online]. Available: http://ngawest2.berkeley.edu/spectras/new?sourceDb_flag=2. [Accessed May 2016].

[13] United States Geological Survey, "Lower 48 Maps and Data," 8 January 2015. [Online]. Available: http://earthquake.usgs.gov/hazards/products/conterminous/. [Accessed 6 February 2015].

[14] S. E. Hough, "Shaking from Injection-Induced Earthquakes in the Central and Eastern United States," *Bulletin of the Seismological Society of America*, vol. 104, no. 5, pp. 2619-2626, 2014.

[15] M. Gallucci, "Oklahoma Earthquake Swarm 2014: Rise In Oklahoma Earthquakes Tied to Fracking Wastewater Has Citizens And Scientists Searching For Answers," 15 July 2014. [Online]. Available: http://www.ibtimes.com/oklahoma-earthquake-swarm-2014-rise-oklahoma-earthquakes-tied-fracking-wastewater-has-1627576. [Accessed 11 Februay 2015].

[16] The Donley Brothers Company, The Donley Book of Sucessful Fireplaces, Cleveland, OH: The Donley Brothers Company, 1936.

[17] Simulia, "ABAQUS 6.13 Documentation," 2013. [Online]. Available: http://bobcat.nus.edu.sg:2080/v6.13/index.html. [Accessed May 2016].

[18] P. B. Lourenco, "Computational Strategies for Masonry Structures," Delft University Press, Delft, Netherlands, 1996.

[19] University of California Berkeley, "OpenSees," University of California Berkeley, 2016. [Online]. Available: http://opensees.berkeley.edu/. [Accessed May 2016].

[20] D. Vamvatsikos and C. A. Cornell, "Incremental Dynamic Analysis," *Eathquake Engineering & Structural Dynamics*, vol. 31, no. 3, pp. 491-514, 2002.

[21] F. Pavel and D. Lungu, "Correlations Between Frequency Content Indicators of Strong Ground Motions and PGV," *Journal of Earthquake Engineering*, vol. 17, no. 4, pp. 543-559, 2013.

[22] J. Bommer and A. Martinez-Pereira, "Strong-motion parameters: definition, usefulness and predictability," in *12th World Conference on Earthquake Engineering, Auckland*, Auckland, NZ, 2000.

[23] M. Raghunandan and A. Liel, "Effect of ground motion duration on earthquake-induced structural collapse," *Structural Safety*, vol. 41, pp. 119-133, 2013.